**Gesellschaft für Anlagen-
und Reaktorsicherheit
(GRS) mbH**

Investigation on
Gas Migration

Technical Barriers Concrete
and Bentonite as well as
Granite of the Surrounding
Host Rock

Gesellschaft für Anlagen- und Reaktorsicherheit (GRS) mbH

Investigation on Gas Migration

Technical Barriers Concrete and Bentonite as well as Granite of the Surrounding Host Rock

Contribution to the Gas Migration Test (GMT) at the Grimsel Test Site

Norbert Jockwer
Herbert Kull
Klaus Wieczorek
with contribution of
Rüdiger Miehe

November 2006

Abstract

Recent re-saturation experiments show in detail the time-dependent development of the water content distribution in bentonite, also considering exclusive re-saturation via water vapour. The VAPMOD code that was developed *ad hoc* to simulate re-saturation via water vapour showed - in comparison with the measurements of re-saturation using liquid water - the strong relevance of the diffusion of water vapour in the pore space to the re-saturation process. Although the dynamics of the re-saturation process had not yet been satisfactorily modelled, the results still suggested that this process could be reproduced with sufficient exactness by improved modelling of local re-saturation.

The present report therefore shows two different ways to approach this target. The first way is to improve the very simple quantitative description of the hydration process in order to achieve with it satisfactory modelling results of re-saturation via water vapour. For this purpose analytical functions were developed from various different re-saturation experiments with water vapour which can be used to indicate the hydration rate as a function of the water content. However, the remaining discrepancies between improved model and experiment show that apart from hydration, the other major process involved in re-saturation – the transport of water within the pore space – may possibly not yet be correctly described.

The second way shows that, assuming realistic simplifications, the balance equation that is used in VAPMOD is consistent with the well-known empirical "diffusion law". An example is used to show that the theoretically derived coefficient yields almost the same value as one obtained empirically. Furthermore, it is also shown by means of another example that contrary to past experience, re-saturation can also be modelled successfully with this simplified balance equation if the inflowing water is under increased hydraulic pressure. The new theoretical approach has thus even the potential to eliminate the deficiencies of the empirical "diffusion law" for non-isothermal conditions.

Table of contents

1   Introduction

Many concepts for repositories intended for the final storage of radioactive or chemotoxic waste include bentonite barriers to protect the waste containers against a corrosive attack of water and to impede a possible release of contaminants. The bentonite is usually emplaced in the repository in dried and compacted form. The re-saturation process needs to be considered as part of the long-term safety assessment of the repository and has therefore been a subject of investigation for quite some time already.

Experiments initially concentrated on the water uptake of the bentonite and its evolution over time. They yielded the empirical result that re-saturation can be well described under laboratory conditions, i. e. at room temperature and under atmospheric pressure, by a Fick's approach. Formally this approach is identical to Fick's Second Law on diffusion processes, the associated coefficient has often misleadingly been referred to in the literature as the "diffusion coefficient".

However, the empirical approach for the re-saturation could not be confirmed by experiments in which pressure or temperature were increased or spatially variable [3]. Subsequently, coupled thermal-hydraulic-mechanical (THM) approaches were more frequently used to model re-saturation. These approaches were based on the assumption that liquid water will spread through the pore space of the bentonite and made use of phenomenological similarities between the hydraulic processes during saturation and the classic two-phase-flow theory. In themselves, they are, however, not fully consistent [10], [11], [12].

More recent re-saturation experiments show in detail the time-dependent development of the water content distribution in bentonite, also considering exclusive re-saturation via water vapour. The VAPMOD code that was developed *ad hoc* to simulate re-saturation via water vapour showed - in comparison with the measurements of re-saturation using liquid water - the strong relevance of the diffusion of water vapour in the pore space to the re-saturation process [13]. (In the following, the term "water" shall be used as a synonym of "liquid water". If water vapour is meant, this shall be stated expressly.)

These results allow a physically completely different explanation of the re-saturation process [14]. According to this explanation, water intrudes into the pore space of the

bentonite following the start of re-saturation and at the same time causes an expansion of the interlamellar space – i. e. swelling in the intrusion area - due to the wetting of the clay minerals. This swelling happens very quickly [20] and reduces the further flow of water up to about the amount of water that evaporates at the interface between water and pore atmosphere. The water vapour forming at the interface then diffuses further through the pore space. As becomes clear in Fig. 1.1, on the one hand this causes liquid water to intrude at a permanent rate into the bentonite, but on the other hand the penetration depth of the liquid phase in the bentonite remains very limited. The experiments of [13] indicate that under laboratory conditions the penetration depth is only about 4 mm.
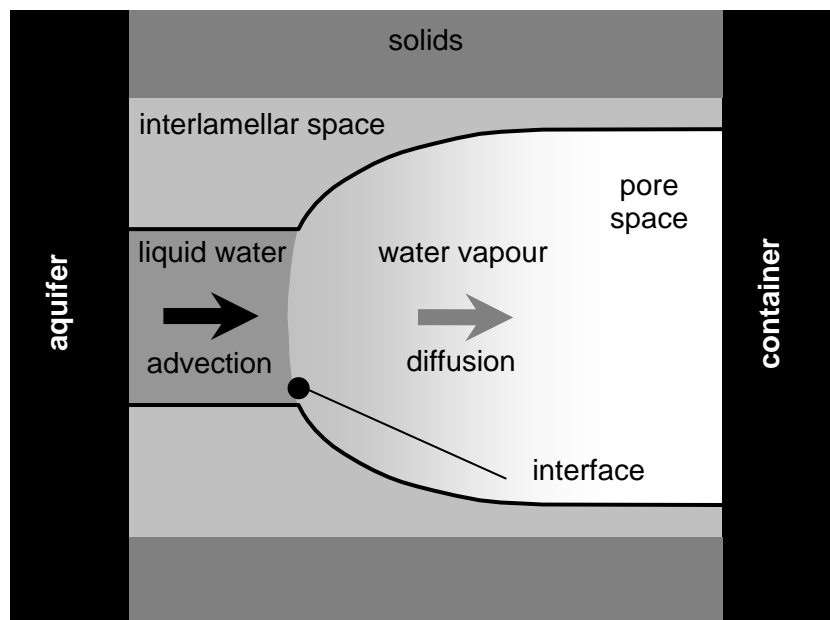
Fig. 1.1　　Schematic diagram of water uptake in the pore space of the bentonite; taken from [15].

Following this initial phase, the bentonite is further re-saturated by the transport of water vapour through its pore space. The swelling process continues until a further expansion of the clay particles is no longer possible for geometric reasons. Only when this process is largely complete will the remaining pore space fill up with liquid water, which is sucked into the bentonite by capillary forces.

In this conceptual model, re-saturation is described by only two processes:

– water vapour transport in the pore space
– hydration in the clay minerals

Water vapour diffusion transports the water into the bentonite body. The gradient in the chemical potential of the mobile, vaporous water in the pore space and of the immobile, hydrated water in the interlamellar space of the clay minerals effects a transfer of water from the pore space into the interlamellar space. This involves swelling of the clay particles, which reduces the porosity. The boundary of this model is formed by the interface between the liquid phase and the air phase. As a boundary condition it is assumed that the atmosphere in this location is saturated with water vapour. These approaches are realised in the VAPMOD code.

It was possible to model the orders of magnitude of the water vapour content distributions in bentonite samples from re-saturation experiments correctly with VAPMOD. Although the dynamics of the re-saturation process had not yet been satisfactorily modelled, the results still suggested that this process could be reproduced with sufficient accuracy by improved modelling of local re-saturation [13]. A vapour diffusion model checked in this way would enable to verify the plausibility of the alternative conceptual model. The present report shows two different approaches to this objective.

The first approach is to improve the very simple quantitative description of the hydration process in order to achieve satisfactory modelling results of re-saturation via water vapour. In this connection, there are two starting points for improvement:

– The approaches implemented in VAPMOD for hydration presuppose a linear dependence between the hydration rate and the gradient between the chemical potential of the water vapour in the pore space and the chemical potential of the interlayer water. According to this, the proportionality factor between the potential gradient and the hydration rate which is referred to here as the "reference hydration rate" (RHR) remains constant. As all other coefficients in VAPMOD are well-known parameters, the only thing that needs to be determined is the RHR. In parallel to the model development, the RHR for unrestrictedly swelling samples at 100 %

atmospheric humidity in the pore space was therefore determined experimentally in [13]. It turned out that the assumption of a constant coefficient only applies approximately. Although the value used in the model calculations was in a plausible order of magnitude, the RHR does in fact decrease with an increasing water content.

– It was furthermore presupposed that a swelling constraint plays no role for the RHR in connection with re-saturation via water vapour. This has not been demonstrated so far. An evaluation of re-saturation experiments from [19] indicates that the hydration rate at constrained swelling depends on the dry density or the degree of precompaction of the bentonite studied. New information provided by [13] from the re-saturation experiments with constricted, compacted bentonite in steel cylinders points in the same direction.

The second approach is to show that, assuming realistic simplifications, the balance equation used in VAPMOD is consistent with the well-known empirical "diffusion law". The balance equation can formally be transformed into Fick's Second Law, with the only remaining coefficient then being quantifiable by known physical parameters. An example is used to show that the theoretically derived coefficient yields almost the same value as one obtained empirically. Furthermore, it is also shown by means of another example that contrary to past experience, re-saturation can also be modelled successfully with this simplified balance equation if the inflowing water is under increased hydraulic pressure.

2 General form of the balance equation

The balance equation for the water in the bentonite is set up in [13] under the assumption that the water is present either as vapour in the pore space or as hydrated water in the interlamellar space. The diffusion of vapour in the pore space then depends on the vapour partial density ρ_v in the pore space and is described by the differential equation (2.1):

$$\frac{\partial(\rho_v \Phi)}{\partial t} - div(\tau \Phi D \cdot grad\, \rho_v) = r_p \qquad (2.1)$$

ρ_v - vapour partial density in the pore space [kg/m³]

Φ - porosity [-]

τ - tortuosity [-]

D - coefficient of binary gas diffusion [m²/s]

r_p - source/sink for the vapour in the pore space [kg/(m³ s)]

t - time [s]

In this context, the sink r_p represents the hydration-induced flow of water from the pore space into the interlamellar spaces of the clay minerals. The density of the hydrated water corresponds to about the density of liquid water [13]. Owing to the big density differences between the vapour in the pore space and the interlayer water, the proportion of water vapour in the water content of the bentonite can therefore be neglected. Thus the water content of the bentonite corresponds with very good approximation to the amount of water stored in the interlamellar space. Hydration changes the amount of water in the interlamellar spaces of the clay minerals according to

$$\rho_d \frac{\partial w}{\partial t} = r_s \qquad (2.2)$$

ρ_d - dry density of the bentonite [kg/m³]

w - water content [-]

r_s - source/sink for the hydrated water [kg/(m³ s)]

As sources and sinks with reversed signs are the same in equations (2.1) and (2.2), the two equations can be summarised as follows:

$$\frac{\partial(\rho_v \, \Phi)}{\partial t} + \rho_d \, \frac{\partial w}{\partial t} - div(\tau \, \Phi \, D \cdot grad \, \rho_v) = 0 \qquad (2.3)$$

In equation (2.3), w and ρ_v are independent variables. A second equation is therefore needed. This may be an equation to quantify the hydration rate. The hydration rate is the specific amount of water that transfers into the interlamellar spaces of the clay minerals per time unit. With the help of the Kelvin equation for the chemical potential, this rate ensues according to [13] as follows:

$$\frac{\partial w}{\partial t} = \dot{\overline{m}} = a \, \frac{RT}{M_w} \ln \frac{r_h}{r_{heq}(w)} \qquad \text{with } r_h = \frac{\rho_v}{\rho_{sat}} \qquad (2.4)$$

$\dot{\overline{m}}$ - specific hydration rate [1/s]

a - proportionality factor [s/m²]

R - universal gas constant [J/(mol K)]

T - temperature [K]

M_w - molecular weight [kg/mol]

r_h - relative humidity [-]

$r_{h\,eq}$ - relative humidity in the thermodynamic equilibrium [-]

ρ_{sat} - vapour saturation partial density [kg/m³]

The relative humidity in the thermodynamic equilibrium $r_{h\,eq}(w)$ is provided by an adsorption isotherm[1].

Equations (2.3) and (2.4) are solved in VAPMOD under the following two assumptions. First, a linear relation is assumed between the difference of the chemical potential and the hydration rate. This leads to a constant proportionality factor a so that the constant variables in equation (2.4) can be summarised to form the reference hydration rate $\dot{\overline{m}}_{ref}$:

---

[1] This has to be taken into account when applying the equation to problems involving variable temperature.

$$\dot{\overline{m}}_{ref} = a\frac{RT}{M_w}$$

(2.5)

$\dot{\overline{m}}_{ref}$ - reference hydration rate [1/s]

Second, in the case of the thermodynamic equilibrium, adsorption isotherms establish a relation between the water content and the relative humidity in the pore space, for the MX-80 e. g. [17], [9]. These adsorption isotherms can be well approximated by a linear approach, except in the range of very high relative humidity levels (95 % - 100 %):

(2.6)

$$w = r_h w_{max}$$

w_{max} - fictitious final water content at r_h=100 % [-]

Such an approach is therefore assumed in VAPMOD.

3 Model comprising re-saturation kinetics

3.1 Determination of the reference hydration rate

Starting point for the determination of the reference hydration rate are the measurements of the water content of bentonite samples in a defined water vapour atmosphere as a function of time. From these data, the hydration rate ensues according to equation (2.4) as derivative with respect to time. With the help of equation (2.5) it is then possible to determine the reference hydration rate $\dot{\overline{m}}_{ref}$ as a function of the humidity and the water content[2].

Two ways offer themselves for determining the hydration rate $\dot{\overline{m}}$. The first, faster one was followed in [13]. Two neighbouring data points i and i+1 each were used to calculate the momentary hydration rate as quotient

$$\dot{\overline{m}}_i\left(\frac{t_{i+1}+t_i}{2}\right) = \frac{w_{i+1}-w_i}{t_{i+1}-t_i}$$

(3.1)

Since the water content is a function of time, it is also possible to present the hydration rate as a function of the water content, which is advantageous with a view to using it in VAPMOD.

This method gives a first impression of the order of magnitude of the hydration rate and its dependence on the water content. However, it also holds uncertainties. Owing to the difference quotient, the inaccuracies in the data points lead to large margins of deviation in the derivative upon the approximation of the differential quotient. In addition, there are also negative gradients in connection with the pointwise evaluation which naturally cannot be contained in the graphic representation. Furthermore, a high density of data is required in connection with the large gradient at the beginning of the observation period.

---

[2] The available re-saturation experiments have so far only been carried out at saturated-vapour pressure. Therefore the re-saturation behaviour determined at full vapour saturation has to be extrapolated to situations with lower humidity. The reliability of this approach remains to be verified.

These difficulties can be bypassed by pursuing the second way, which involves looking for an analytic function for $w(t)$ by means of a data fit. The derivative of this function with respect to time then provides a continuous function for the sought-after mass flow $\dot{\overline{m}}$. In the following, the functions determined pointwise as well as the analytically determined functions are presented.

3.1.1 Water content as a function of time

Fig. 3.1 shows the time history of the water content in the experiments of [13] with freely swelling samples. These consisted of bentonite powder as well as of compacted bentonite discs with a dry density of about 1500 kg/m³. The double-logarithmic representation shows a certain variation in the measuring results. Still, it can be clearly seen that the re-saturation speed slows down above a water content of about 20 %. At microstructure level, a water content of 20 % in MX-80 corresponds to the re-saturation up to a bimolecular layer of water molecules in the interlamellar spaces of the clay minerals [9].
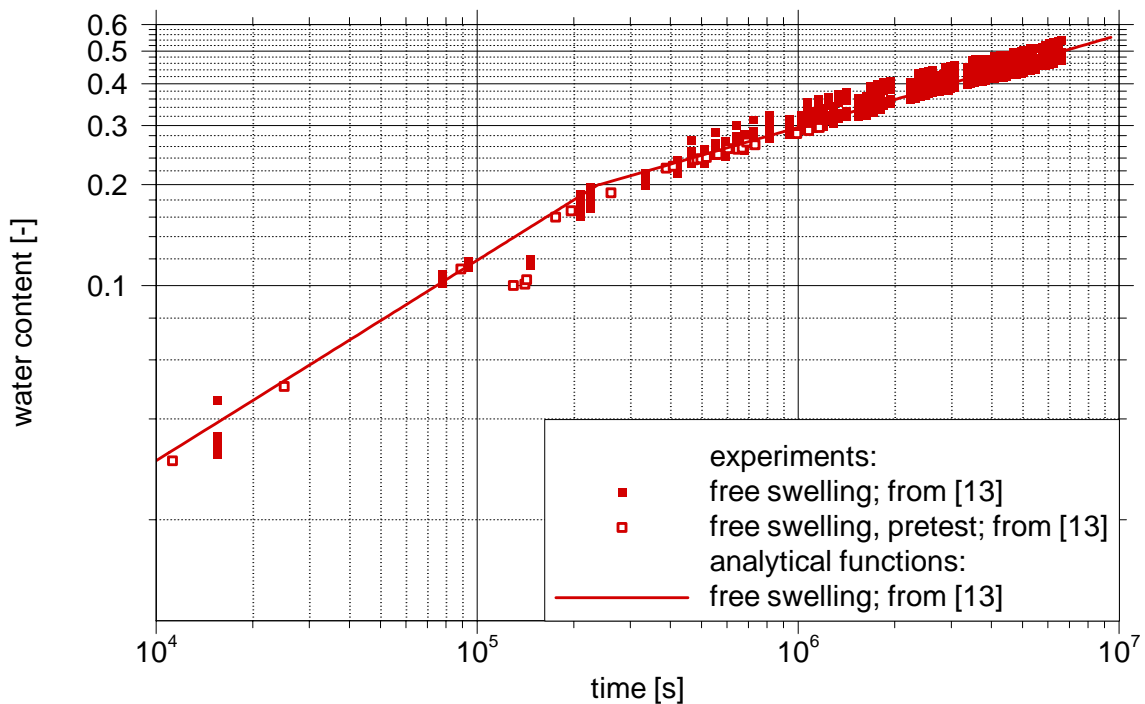

Fig. 3.1 Water content as a function of time at freely swelling samples according to [13].

The piecewise linear distribution in the graph of the analytic function can be described by exponential functions of the type

$$w(t) = b \cdot t^a$$

(3.2)

Here, the distribution parameters ensue as

$$b = \frac{w_i}{t_i^a}$$

(3.3)

for any point i through which the curve is to run and as

$$a = \frac{\log w_q - \log w_p}{\log t_q - \log t_p}$$

(3.4)

for the two points p and q which characterise the gradient of the straight line on a double logarithmic scale. The analytic curves plotted in Fig. 3.1 ensue from the parameters

$a = 0.5981$, $b = 0.0001215$ for $w < 0.20$ and

$a = 0.2759$, $b = 0.006551$ for $w > 0.20$.

The time history of the water content in connection with the re-saturation of MX-80 is qualitatively confirmed by the measurements in [9] and [19]. In [9], data were acquired across a wide spectrum of water content for three different test bodies of different degrees of pre-compaction and different sizes. When evaluated in the same way, it turns out that the piecewise constant water uptake is the same in all samples. The transition between the linear sections, however, lies at a slightly lower water content. The re-saturation speed, too, is apparently lower. It is unclear what the dry densities of the samples were. According to the experiment description, the bentonite was filled into small bowls and "pressed on slightly". In the associated illustration, however, the dry densities are given as 1350 kg/m³ and 1770 kg/m³.

As was already the case in the tests in [13], there is no discernible dependence on the degree of compaction of the samples. However, Fig. 3.2 shows clearly lower values for the slightly larger test body. The reason for this is not clear. Still, this result would be

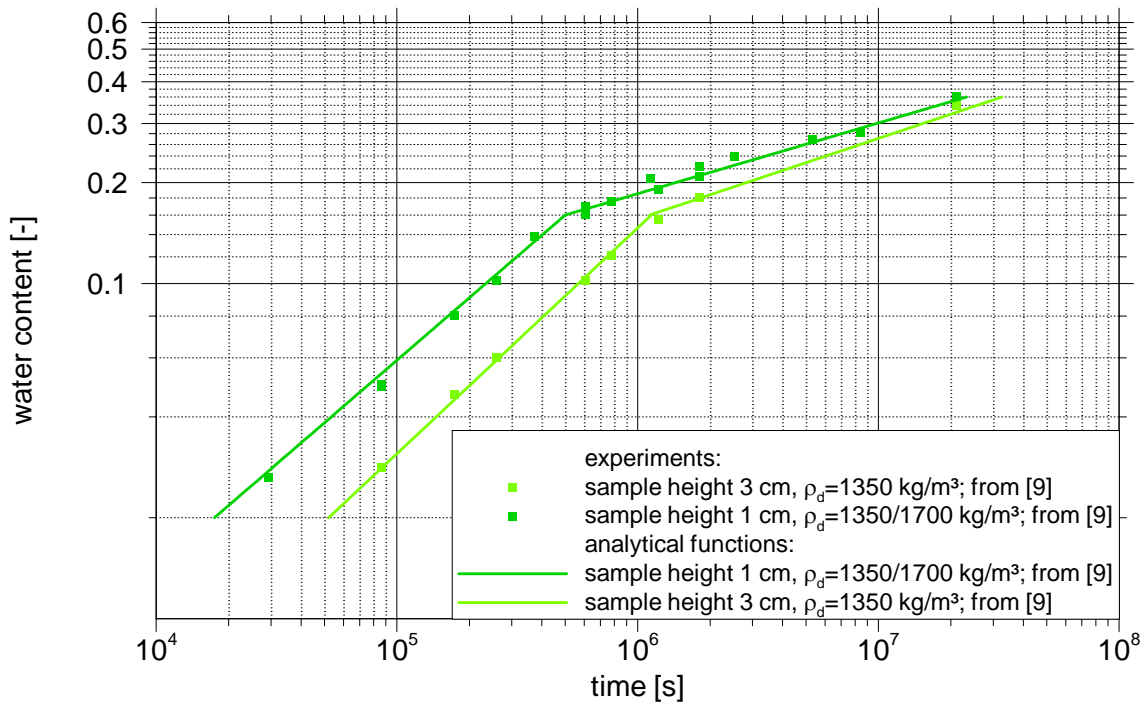consistent with a certain swelling constraint of the samples, as shown in the following in the example from [19].

Fig. 3.2   Time-dependent water content according to [9].

The re-saturation tests described in [19] were also carried out with samples with varying degrees of compaction, but fully constrained from swelling. The results shown in Fig. 3.3 show clearly that in this case the water uptake depends on the degree of compaction.

Data density in this example is low. Only one measuring point each for the slightly and the strongly compacted sample lies below the water content level of 20 %. These points again are clearly off the trend of the remaining data points. Here, it is assumed *ad hoc* that in this case, too, the water uptake velocity is higher at low saturation levels than at higher saturation levels. Under the condition that the average hydration rate at low water content corresponds to about the velocity given in Fig. 3.2 for this area, the plotted straight interrupted lines shown in Fig. 3.3 ensue. Here, too, the hydration rate would change accordingly at about 20 %. However, as the plotted straight interrupted line sections have not been validated, they are not considered any further in the following.
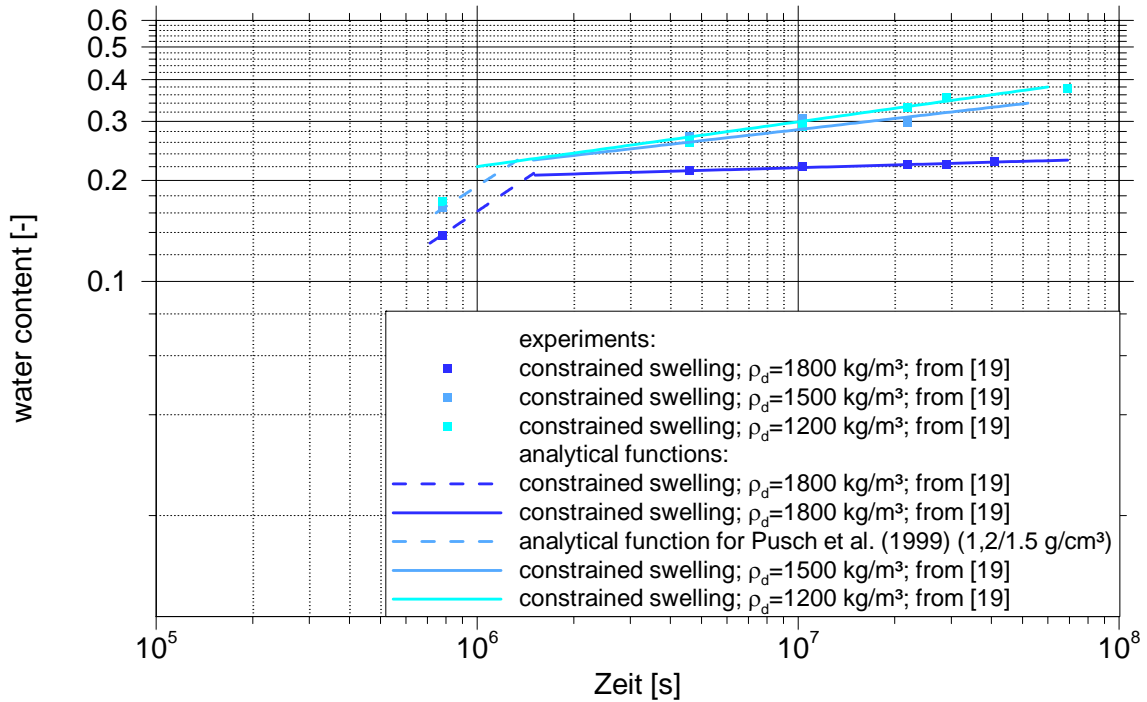
Fig. 3.3   Time-dependent water content according to [19].

In [13], experiments with vapour and swelling-constrained samples were carried out with the aim to establish the spatial and time-dependent development of the water content upon re-saturation. The samples had an initial dry density of ρ_d = 1500 kg/m³. These experiments can also be used for describing the re-saturation dynamics of a swelling-constrained sample. For this purpose it is assumed by approximation that the relative humidity in the area of the bentonite bordering immediately on the vapour reservoir is 100 %. The average water content in the about 3-mm-strong edge zone of the test bodies is shown in Fig. 3.4 as a function of time. The two sections with different re-saturation velocities do not differ as clearly here as in the previous examples, but a transition is also discernible in this case, lying again at a water content level of about 20 %. Using the respective parameters a and b, the analytical curves ensue as follows:

a = 0.1232, b = 0.03146 for w < 0.20 and

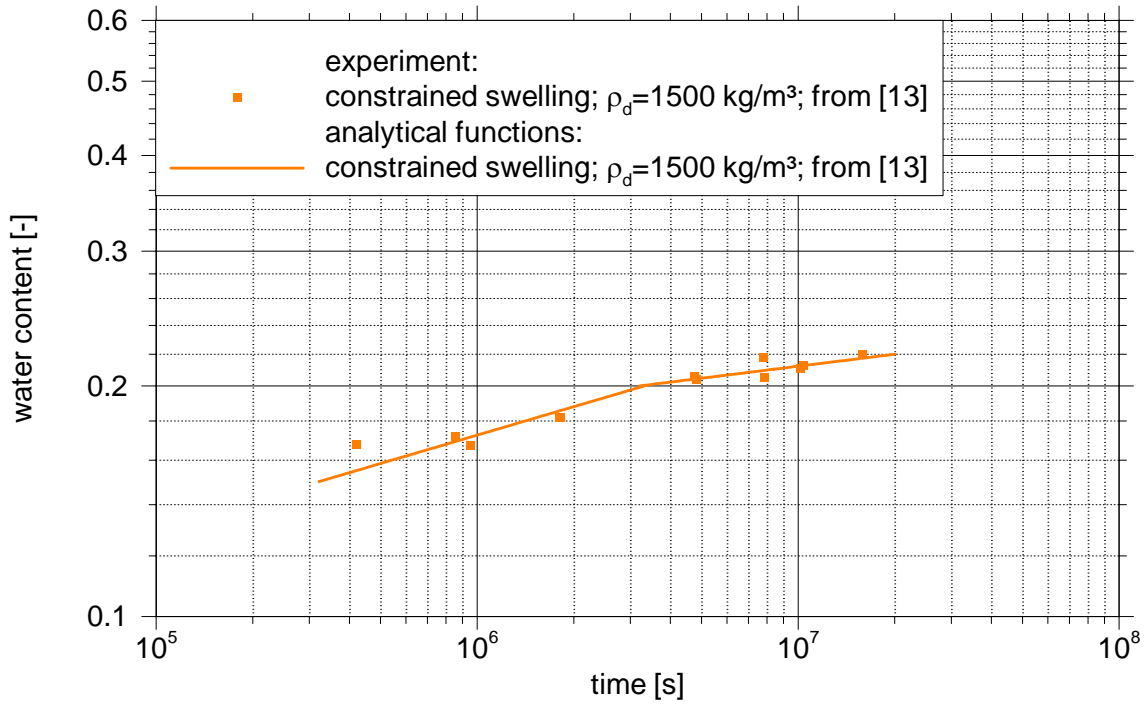a = 0.05201, b = 0.09177 for w > 0.20

Fig. 3.4 Time-dependent water content of swelling-constrained samples according to [13].

In summary it can be stated that the time history of the water content cannot apparently be described with a simple analytic function. The results furthermore point at the so-far neglected circumstance that the re-saturation velocity of swelling-constrained samples may depend on the degree of compaction. In this case it would have to be analysed what causes this dependence.

3.1.2 Hydration rate as a function of the water content

Using (3.2) once more, the derivative of (3.2) with respect to time provides the following analytic function for the hydration rate:

$$\dot{\bar{m}} = ab\left(\frac{w}{b}\right)^{\left(1-\frac{1}{a}\right)} \qquad (3.5)$$

As the function w(t) is not mathematically smooth at the kink, there is a discontinuity in the derivative, as shown in Fig. 3.5. This is unlikely to correspond to the actual conditions but is rather a rough approximation to a fast transition.

A comparison with the pointwise evaluation shows that the inaccuracies in the approximation of the derivative by difference quotients especially above w = 20 % lead to an over-estimation of the hydration rate. Still, both evaluation methods clearly show an influence of the degree of compaction on the water-content-dependent hydration rate.
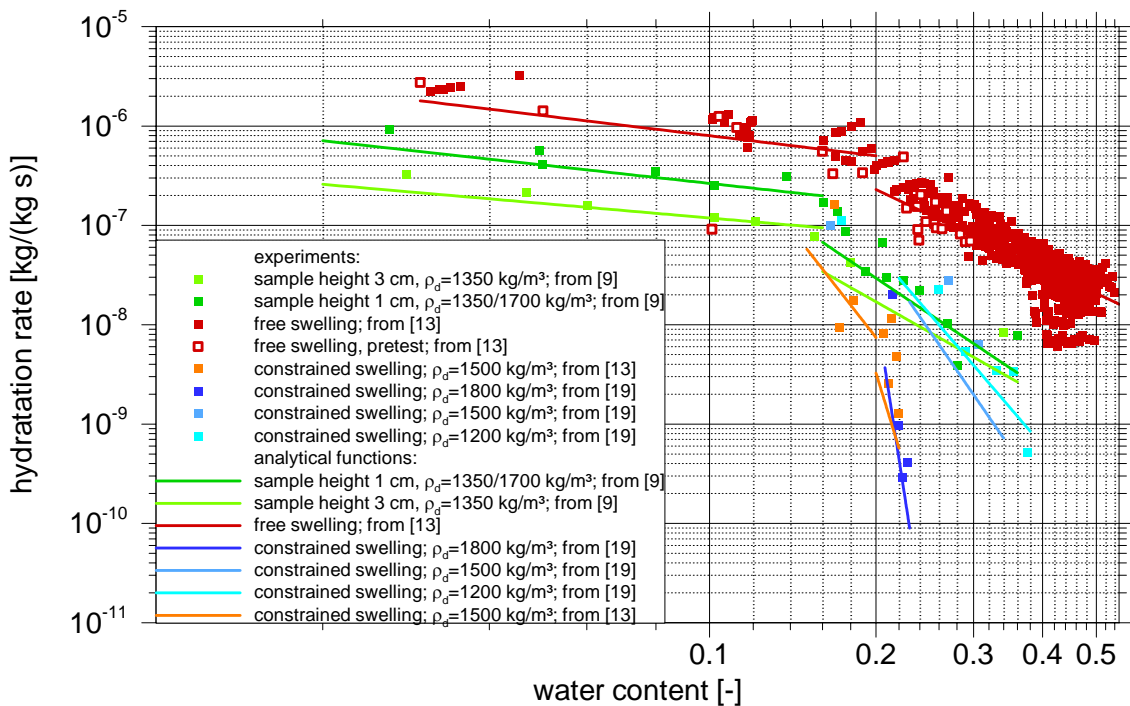

Fig. 3.5   Hydration rate as a function of the water content in samples according to [9], [19] and [13].

What is striking is the good agreement of the swelling-constrained samples from [19] with a dry density of 1800 kg/m³ and those from [13] with a dry density of 1500 kg/m³. It may be that the term "dry density" is used differently in the two sources. While dry density in [13] refers to material that was dried at 105 °C for 24 hours, this parameter is not explained any further in [19]. In the literature it is, however, not unusual to apply the notion of dry density to air-dry bentonites that already have a water content of 8 % to 10 %. In this case, the dry density given in [19] as 1800 kg/m³ would correspond to a

density of about 1650 kg/m³ following oven-drying at 105 °C. This would explain the close proximity of the data for the hydration rate.

The fact that the water uptake rate in the experiments of [9] does not depend on the degree of compaction initially speaks on the one hand for an experiment with unconstrained swelling. On the other hand, the systematically lower rate in connection with samples of greater height indicates a certain constraint. This constraint would also explain the overall lower uptake rates in the experiments in [9] compared with the results in [13]. Additionally, the data points (and curves) in [9] and the swelling-constrained samples according to [19] are also very close at dry densities of 1500 kg/m³ and 1200 kg/m³, respectively. If one assumes once more that in [19] the term "dry density" is actually used to describe the air-dry bentonite, the density ensuing after oven-drying the samples would be 1363 kg/m³ and 1090 kg/m³, respectively. At these density values, any major swelling constraint will only occur at a higher water content due to the high porosity levels. The data in [9] as well as the data for the low- and medium-compacted bentonite in [19] are therefore consistent with a slight swelling constraint.

3.1.3   Reference hydration rate as a function of the water content

The application of equations (2.5) and (2.6) in equation (2.4) yields a conditional equation for the reference hydration rate:

$$\dot{\bar{m}}_{ref} = \frac{\dot{\bar{m}}}{\ln \dfrac{w_{max}}{w}} \quad \text{for} \ \ r_h=1 \tag{3.6}$$

At $w_{max}=0.32$, the data points and curves in Fig. 3.5 result in the associated reference hydration rates given in Fig. 3.6.

For a water content below 16 % to 20 %, the assumption of the linearity between potential difference and hydration rate and thus the assumption of a constant reference hydration rate is apparently approximately correct. Here, the RHR lies between 10^{-7} 1/s and 10^{-6} 1/s.

In the case of the non-swelling-constrained samples in [13] (data points and curves shown in red) and the samples in [9] (data points and curves shown in green), the RHR is approximately constant even for higher water contents, albeit at a slightly lower level (between about $7 \cdot 10^{-7}$ 1/s and $7 \cdot 10^{-8}$). The values for the low- and medium-compacted samples in [19] (data points and curves shown in light and medium blue) lie in between at about $2 \cdot 10^{-7}$ 1/s.
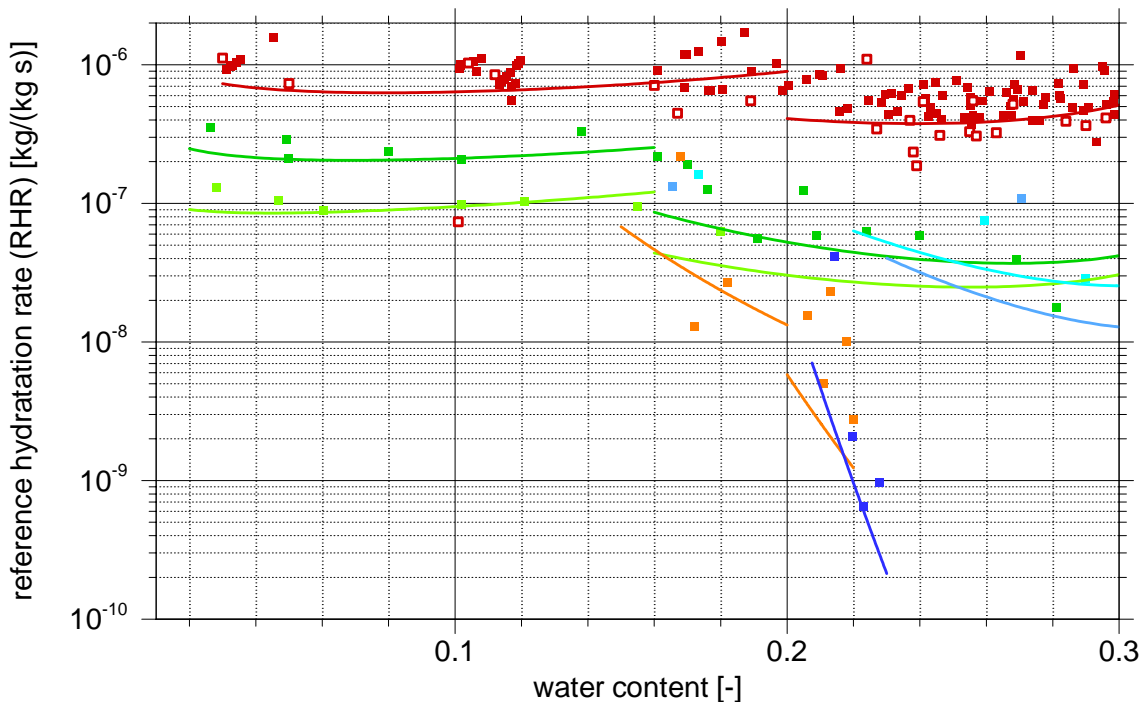

Fig. 3.6   Reference hydration rates as functions of the water content in samples in [9], [19] and [13]; square symbol: measurement, line: calculation; colour-coding:

        — sample height 1 cm, ρ_d=1350/1700 kg/m³; from [9]
        — sample height 3 cm, ρ_d=1350 kg/m³; from [9]
        — free swelling; from [13]
        — constrained swelling; ρ_d=1500 kg/m³; from [13]
        — constrained swelling; ρ_d=1800 kg/m³; from [19]
        — constrained swelling; ρ_d=1500 kg/m³; from [19]
        — constrained swelling; ρ_d=1200 kg/m³; from [19]

In contrast, the RHRs of the highly compacted sample in [19] (data points and curves shown in dark blue) as well as of the swelling-constrained sample in [13] (data points and curves shown in orange) deviate clearly from the other results. Nevertheless, they lie closely together, as was already the case with the hydration rate in Fig. 3.5. An

increase of the water content by a few percent causes the RHR to drop by one and a half orders of magnitude from $3 \cdot 10^{-8}$ 1/s to $8 \cdot 10^{-10}$ 1/s.

3.2 Comparison of modelling and measuring results

3.2.1 Constant reference hydration rate

In [13], a re-saturation experiment is described involving water vapour and full swelling constraint. It provides the time history of the water content distribution in a 10-cm-long cylindrical MX-80 bentonite body. This experiment was modelled with VAPMOD using a constant reference hydration rate of 10^{-7} 1/s. The comparison of measured data and modelling results is shown in Fig. 3.7. This revealed first that the re-saturation at the inflow boundary in the model initially takes place too slowly but later on too fast. Second, the full-scale value at the inflow boundary of the model is apparently too high. The representation of the water content at the inflow boundary - i. e. approximately at maximum vapour saturation - in Fig. 3.8 indicates a full-scale value of approx. w = 24 %. This corresponds to a final porosity of about 14 %. An improvement of the model in [13] has to take these circumstances into account.
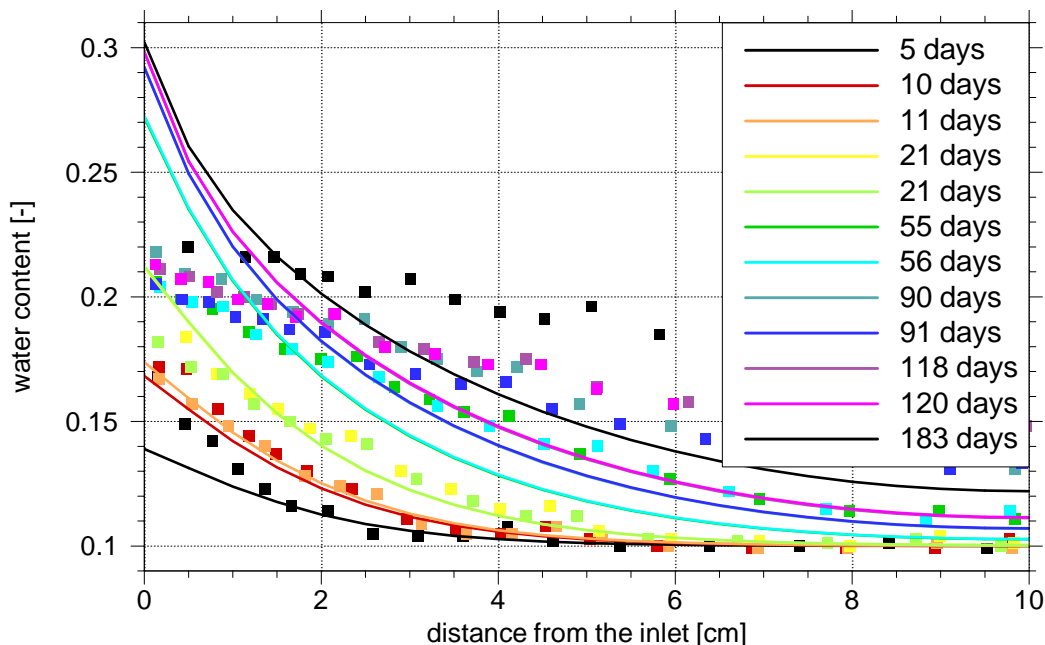

Fig. 3.7   Measured data and modelling results in [13] concerning re-saturation
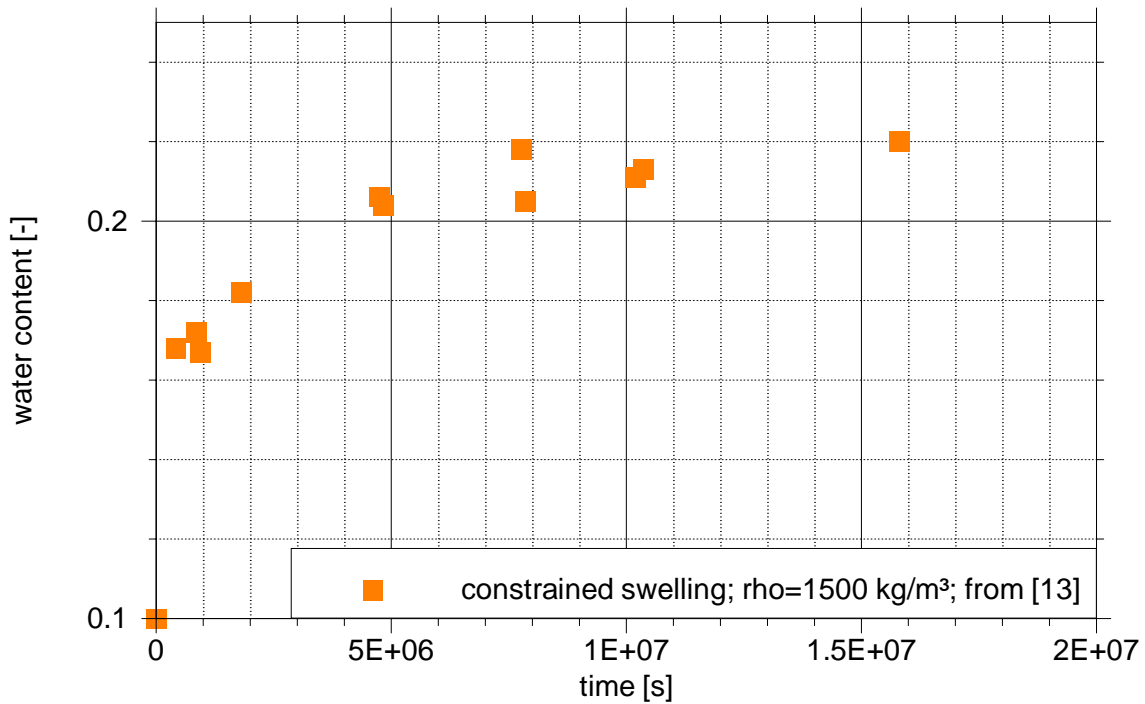via vapour; square symbol: measurement, line: calculation.

Fig. 3.8   Time-dependent water content at the inflow boundary in [13].

3.2.2   Calibrated reference hydration rate

The strong changeability of the RHR with the water content that can be seen in Fig. 3.6 could explain why the model with constant RHR used so far cannot simulate the re-saturation experiment in [13] to complete satisfaction. However, there have been no investigations yet as to what effects this changeability can cause.

Still, the simulation of a special experiment is nevertheless possible if one calibrates the hydration rate with the data of this experiment instead of considering all physical processes that influence the hydration rate. In this case, less physical understanding is required for the modelling. Although the calibrated data will then no longer be transferable, the reliability of the model assumptions can be verified up to a certain degree.

In order to simulate the re-saturation experiment with water vapour of [13], the analytical functions adapted to the data are inserted for the RHR in equation (2.4). Here, the same parameters are used that have already also been the basis for Fig. 3.4 in Ch. 3.1.1. Since the hydration rates are calibrated with the measured data at the inflow

boundary, measured and modelled data at this point have to be in agreement. The results of the improved model in Fig. 3.9 show that compared with the experimental results, this is actually so. For the first three weeks, the measuring points are modelled well even in the further course of the curves, although the model curves show a turning point from the start. However, the modelled curves for later points in time remain behind the measured results at a distance of more than 3 cm from the inflow boundary.
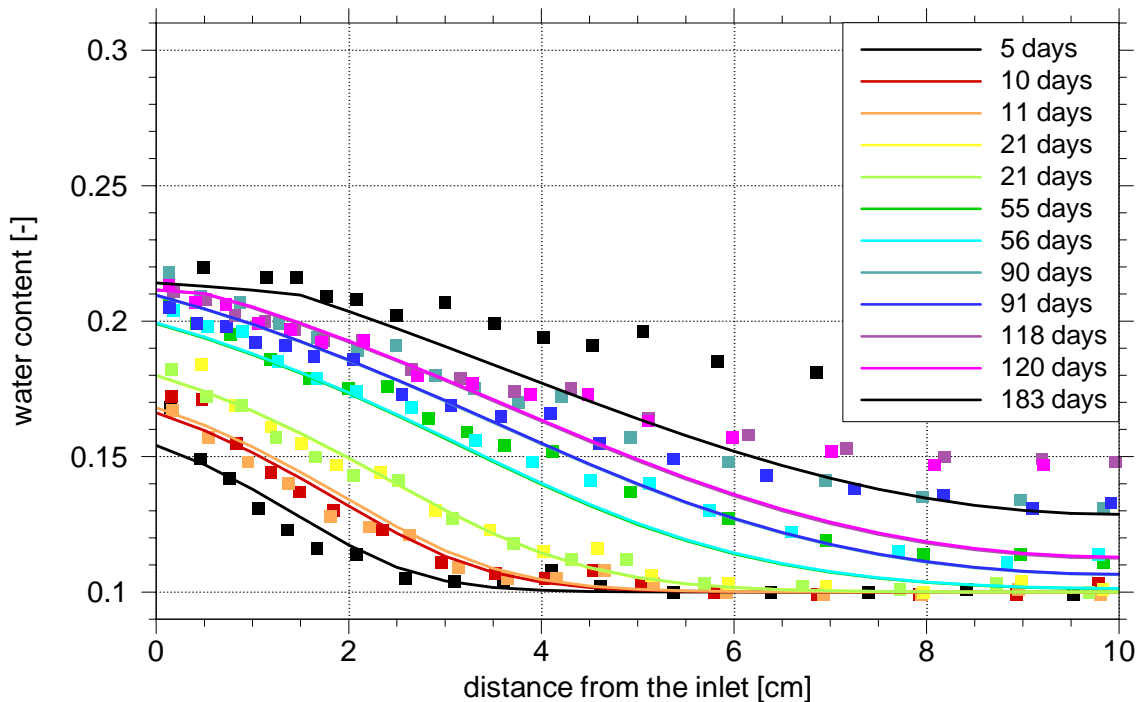

Fig. 3.9   Results with calibrated hydration rates;
                 square symbol: measurement, line: calculation.

All in all, the new model yields clearly better results than the model with a constant RHR. At the same time, however, it shows up gaps in the understanding of the re-saturation process. It is still unclear why the water content in the model's far side of the inflow boundary remains behind the measurements. It appears that either the vapour transport in the pore space or the hydration process is not sufficiently described.

In [13] the possibility has already been indicated that the effect of the Knudsen diffusion could cause an increased water transport due to the narrowing pore channels. As this effect is mainly expected in the area of advanced re-saturation in proximity to the inflow

boundary, the area further removed from the inflow boundary would therefore be subjected to a higher water supply, which would speed up hydration there.

It has so far not been investigated either whether the correlation between RHR and water content, which is presently only known for relative humidities of about $r_h{\sim}1$, applies in the same way to lower humidities. Should this not be the case, then this could also be an explanation of the deviation of the model results from the experiment.

3.3   Conclusions

The evaluation of various experiments on the re-saturation of bentonite via water vapour yields no clear function for water uptake as a function of time. Thus it is also not possible to derive a clear function for the hydration rate as a function of the water content. The compaction of the samples has no influence on water uptake in the case of the freely swelling samples [13]. However, it appears that any constraint to swelling reduces the hydration rate considerably. The cause of this phenomenon remains to be clarified.

The modelling of re-saturation via vapour with calibrated hydration rates leads to a better agreement of the experiment and modelling results than using the theoretical ad-hoc approaches [13]. The fact that the modelling results are nevertheless not satisfactory raises some questions with regard to the two essential effects in connection with the isothermal re-saturation of bentonite via water vapour:

– Vapour transport in the pore space
  • How strong is the influence of Knudsen diffusion on vapour transport?
  • How can Knudsen diffusion be described in the model?

– Hydration
  • What influence does the precompaction of the bentonite have on the hydration rate at constrained swelling? What effects play a role in this context?
  • How high are the hydration rates in an only partially saturated vapour atmosphere?

Until these questions are answered, the VAPMOD code will not be able to predict accurately the dynamics of re-saturation via vapour. This means that at the current state

of development, the question of what part vapour diffusion plays in re-saturation when a bentonite is in contact with liquid water cannot be answered conclusively. Still, the very simple approaches in VAPMOD are already capable of roughly approximating the actual conditions.

4   Model with equilibrium hydration

In the preceding chapter, the phenomenon of bentonite re-saturation via water vapour was analysed to show the dominance of water vapour transport over the transport of liquid water. For the same purpose, the following will deal with re-saturation as a result of a contact with liquid water. These analyses are based on the re-saturation experiments with liquid water in [13].

4.1   Process velocities

The starting point of the considerations are model calculations made with VAPMOD in which the reference hydration rate and therefore the ratio of the process velocities of vapour transport and hydration are varied [1]. In the range of realistic RHRs, the results are little sensitive to a variation of the RHR. Also, the admissible time step becomes smaller the more the RHR increases. These two observations suggest that the dynamics of re-saturation via water vapour are governed more by the water vapour supply than by the hydration rate. In other words, hydration would be a much faster developing process than vapour diffusion, so that locally an equilibrium of humidity and hydrated water would establish itself very quickly.

The same conclusion can be derived from an evaluation of the model calculations with VAPMOD that simulate the re-saturation experiments with liquid water in [13]. Fig. 4.1 shows the comparison of the water content distributions of the measurement and the simulation. In the model, an RHR of $\dot{m} = 10^{-7}$ 1/s was used. The initial re-saturation with liquid water, which sets in temporarily at the start of the re-saturation process as a result of the capillary forces, is taken into account by moving the inflow boundary in the model 4 mm towards the centre of the area.

Apart from the water content, which after all mainly represents the hydrated interlayer water, VAPMOD also provides the equilibrium water content belonging to the humidity. According to (2.4), the ratio between the theoretical equilibrium water content and the prevailing water content is a measure for the difference of the chemical potentials of pore water and interlayer water. At a ratio of 1, the two potentials are equal, and a local, thermodynamic equilibrium prevails.
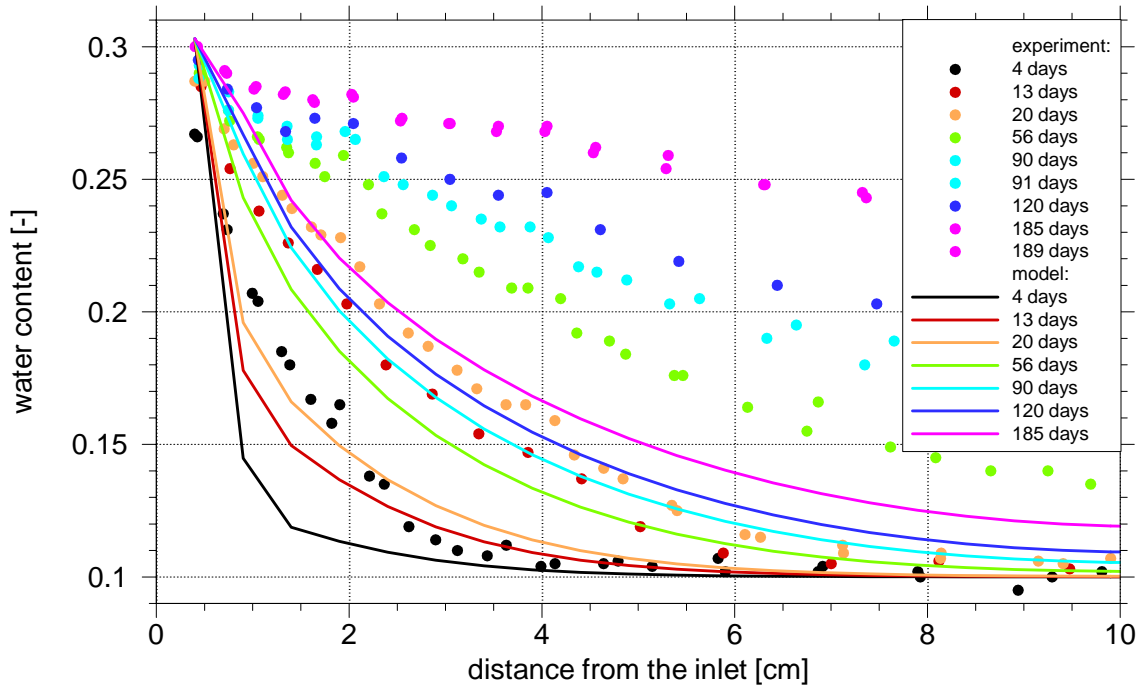
Fig. 4.1   Uptake of liquid water and results of modelling with VAPMOD.

Fig. 4.2 shows the prevailing water content and the equilibrium water content together for the model with $\dot{\overline{m}} = 10^{-7}$ 1/s. The values of the corresponding water content distributions differ from the start by no more than 40 %, and with progressing re-saturation this difference quickly becomes smaller. However, as can be seen from the compilation of RHRs in Fig. 3.6, at the beginning of re-saturation the RHR might also have had a value of $\dot{\overline{m}} = 10^{-6}$ 1/s. In this case, the approximation to the state of equilibrium would be far advanced from the start, as Fig. 4.3 shows in analogy to Fig. 4.2.
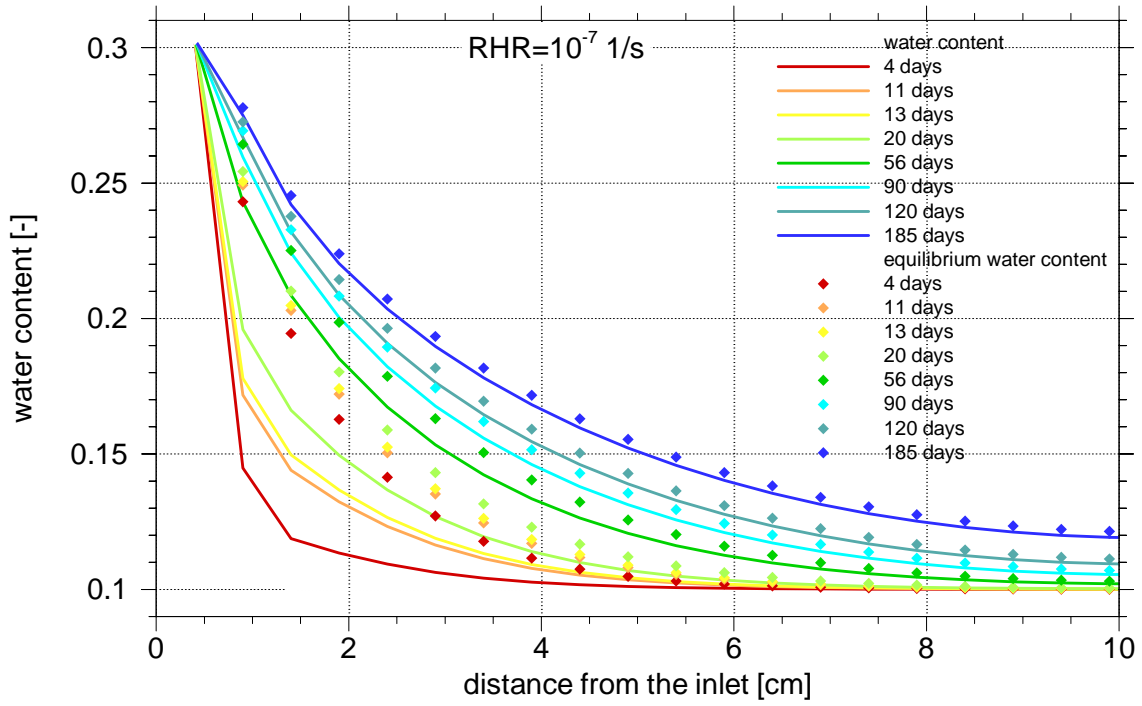
Fig. 4.2   Water content and equilibrium water content at $\dot{\overline{m}} = 10^{-7}$ 1/s.
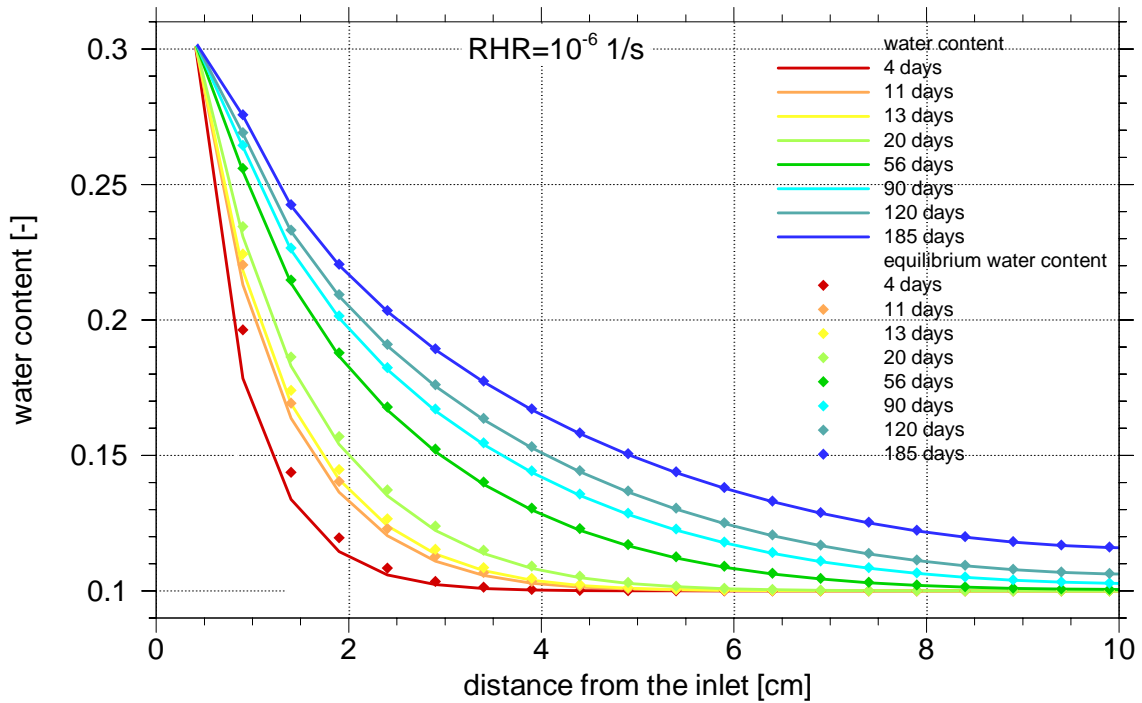

Fig. 4.3   Water content and equilibrium water content at $\dot{\overline{m}} = 10^{-6}$ 1/s.

25

4.2   Simplified balance equation

The results of the sensitivity analysis in [1] as well as the direct evaluation of VAPMOD modelling results appear to justify a simplification of the balance equations derived in Section 2 under the assumption of equilibrium hydration. This means that in the mathematical model, an instantaneous equilibrium between the amount of hydrated water and the vapour partial pressure is assumed by approximation. Via equation (2.6) one then arrives at a linear-proportional relationship between water content and vapour partial pressure

$$w = \frac{w_{max}}{\rho_{v\,sat}} \rho_v \qquad (4.1)$$

with which one independent variable in balance equation (2.3) can be eliminated:

$$\frac{\partial(\rho_v \Phi)}{\partial t} + \frac{\rho_d w_{max}}{\rho_{v\,sat}} \frac{\partial \rho_v}{\partial t} - div(\tau \Phi D \cdot grad\, \rho_v) = 0 \qquad (4.2)$$

In equation (4.2) the changeability of the porosity with time also has to be considered. Compared with the time derivative of the vapour partial pressure, however, this contribution is low and can be neglected [13]. Against this background it is also assumed that the dependence of the tortuosity as well as of the porosity on the water content can also be neglected for the further considerations. Although porosity as well as tortuosity may possibly decrease with progressing re-saturation, this is fronted by a possible simultaneously developing transition from free diffusion of the vapour in the pore space to Knudsen diffusion. Formally, this results in an increase of the diffusion coefficient.[3] Insofar, the product of porosity, tortuosity and the coefficient of the binary gas diffusion during re-saturation is assumed to be constant.

---

[3] This transition takes place when the mean free path length of the diffused molecules lies in the order of magnitude of the pore diameter. The mean free path length of water molecules in air is approx. 100 nm (e. g. [13]). According to [16] (cited in [6]), the Knudsen diffusion is without relevance only at a pore diameter above 1 µm. However, a large proportion of the pore channels in compacted MX-80 bentonite has a diameter of less than 1 µm [8], [19], [21]. These indications make the occurrence of Knudsen diffusion appear likely.

With this simplification and due to a restriction to only one dimension, equation (4.2) has the following form:

$$\left(\Phi + \frac{\rho_d w_{\max}}{\rho_{v\,sat}} \right) \frac{\partial \rho_v}{\partial t} - \tau \, \Phi \, D \frac{\partial^2 \rho_v}{\partial x^2} = 0 \qquad (4.3)$$

The first bracket term in equation (4.3) can be considered as a retardation coefficient R_d:

$$R_d = \Phi + \frac{\rho_d w_{\max}}{\rho_{sat}} \qquad (4.4)$$

R_d -   retardation coefficient [-]

and eventually transforms equation (4.3) into the form

$$\frac{\partial \rho_v}{\partial t} - D_{th} \frac{\partial^2 \rho_v}{\partial x^2} = 0 \quad \text{with} \quad D_{th} = \tau \, \Phi \, \frac{D}{R_d} \qquad (4.5)$$

D_{th} -   diffusion coefficient of the simplified balance equation [m²/s]

This equation corresponds formally to the empirical "diffusion law", a Fick's approach with constant coefficient:

$$\frac{\partial w}{\partial t} - D_{emp} \frac{\partial^2 w}{\partial x^2} = 0 \qquad (4.6)$$

D_{emp} -   empirical "diffusion coefficient" [m²/s]

It has been known of this empirical "diffusion law" for some time that the time-dependent water uptake is described well under laboratory conditions. The range of the values for the empirical "diffusion coefficient" D_{emp} that were derived from laboratory experiments with MX-80 bentonite is remarkably narrow, amounting to hardly more than one order of magnitude [2], [9], [4], [7], [18]: $1 \cdot 10^{-10}$ m²/s $< D_{emp} < 3 \cdot 10^{-9}$ m²/s. However, the empirical "diffusion law" was not confirmed for experimental conditions that deviated from the laboratory conditions, in particular at deviation from room temperature [3].

The independent variables in the two corresponding equations (4.5) and (4.6) – vapour partial pressure in the newly developed balance equation and water content in the empirical "diffusion law" – differ according to equation (4.1) only by one constant factor. By the physically justified approach for the transport of water in the pore space, one therefore arrives at qualitatively the same description of re-saturation as by the evaluation of the experiments involving liquid water.

4.3 Determination of the "diffusion coefficient"

4.3.1 Determination by data adjustment

The balance equation (4.5) and the empirical "diffusion law" (4.6) differ only in the quantity of the coefficient of the spatial derivative, i. e. in the quantity of the "diffusion coefficient". For a comparison of the coefficients D_{emp} and D_{th}, the example of the re-saturation experiment with liquid water in [13] is used again as it yields not only the already frequently analysed water uptake rates but also the far less well known time-dependent water content distribution within the bentonite.

Since according to [5] analytical solutions exist for equations (4.5) and (4.6) – this is described in detail in [12] – it suffices to evaluate the solution for discrete points in space and time. The water uptake rates can be modelled very well with a coefficient of D_{emp} = 3.5·10^{-10} m²/s, as shown in Fig. 4.4. The value lies within the spectrum of the experimentally determined empirical "diffusion coefficient" (cf. Ch. 4.2) and confirms once again the reproducibility of the empirical "diffusion law".

With the empirical "diffusion law" it is also possible to calculate the associated time-dependent water content distributions. Fig. 4.5 shows the distributions ensuing from D_{emp} = 3.5·10^{-10} m²/s in comparison with the measuring results. The good agreement of measurement and model calculation confirms with even more clarity than [2] that the empirical "diffusion law" can describe not only the water uptake but also the dynamics of the water content distribution inside the bentonite. What is decisive in this case, however, is that owing to the formal similarities of the equations this agreement applies in the same way to the balance equation (4.5) which explains the water transport in the pore space exclusively by vapour diffusion.
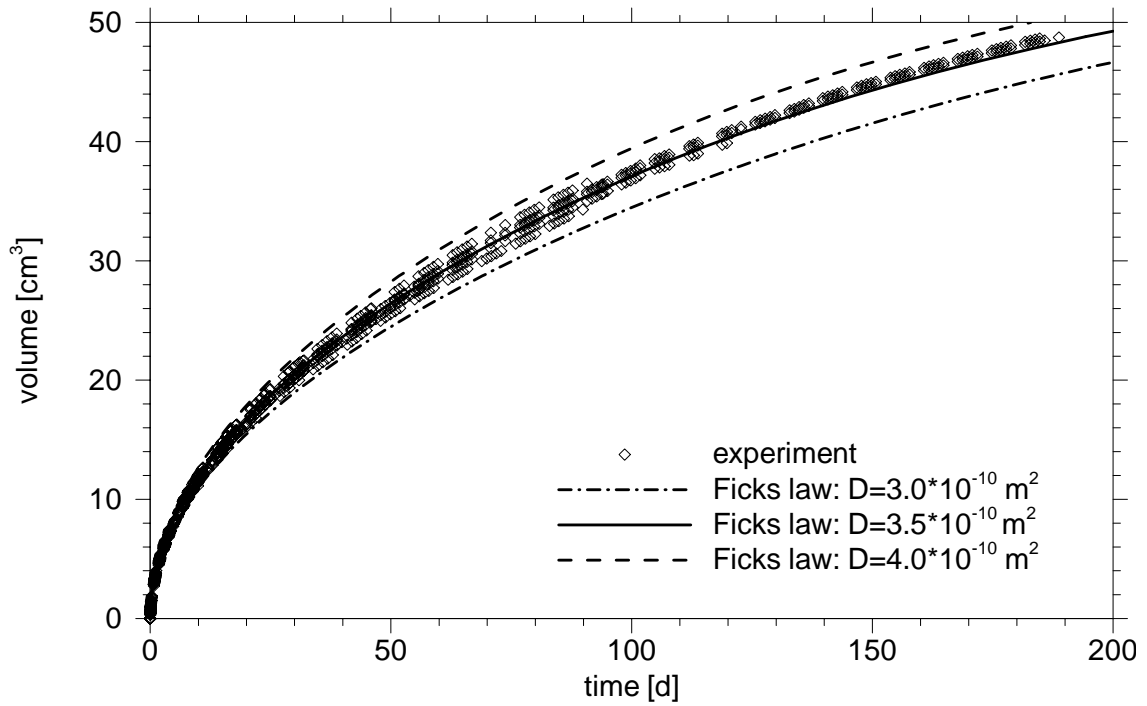
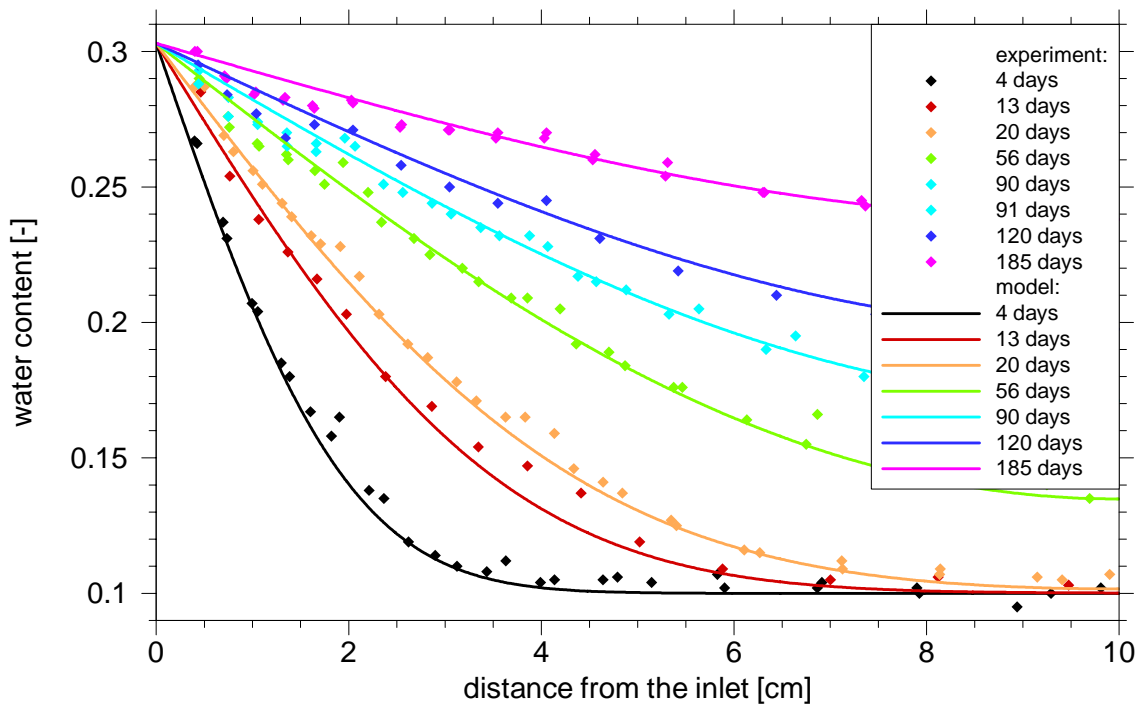**Fig. 4.4**   Water uptake rate: measured data in [13] and "diffusion law".

Fig. 4.5   Water content distributions: measured data [13] and "diffusion law".

4.3.2 Determination by calculation

The parameters required for the estimation of the coefficient D_{th} in the balance equation (4.5) are summarised in Tab. 4.1. These data yield the value $D_{th} = 1.3 \cdot 10^{-10}$ m²/s, which is only slightly lower than the empirical "diffusion coefficient" of $D_{emp} = 3.5 \cdot 10^{-10}$ m²/s obtained for the same experiment. The coefficient D_{th} also lies within the range of the experimentally determined empirical "diffusion coefficients". The "diffusion coefficient" which so far could only be determined empirically can therefore also be obtained theoretically with the help of the re-saturation model based on vapour transport.

Tab. 4.1   Parameters for the estimation of the diffusion coefficient Dth.

Parameter	Value	Dimension
Porosity Φ	0.3	-
Dry density ρ_d	1500	kg/m³
Fictitious maximum water saturation w_{max}	0.32	-
Saturation vapour partial density $\rho_{v\,sat}$	0.0165	kg/m³
Tortuosity τ	0,5	-
Coefficient of binary gas diffusion D [4]	$2.42 \cdot 10^{-5}$	m²/s

4.4 Verification of the VAPMOD code

In the VAPMOD code, hydration kinetics are implemented such that the porosity decreases with an increasing water content, while tortuosity and the diffusion coefficient remain constant. In contrast, the simplification of the balance equation (4.3) described in Ch. 4.2 leads to the product of porosity, tortuosity and diffusion coefficient being constant when equilibrium hydration is assumed in the modelling. The value of the diffusion coefficient thus increases with decreasing porosity. This feature was implemented in VAPMOD by way of trial. With the thus modified VAPMOD code several

---

[4] according to [22] (cited in [6]) for a temperature of 20°C.

calculations were repeated that had already been performed with the analytical solutions for the empirical "diffusion law" and thus for the simplified balance equation.

There was no noteworthy deviation of the results of the modified VAPMOD models from the results obtained with the simplified balance equation. This is a verification of the VAPMOD code as it means that comparison with an analytical solution is possible. Furthermore, the results also confirm the assumption of fast hydration.

5   Increased hydraulic water pressure

5.1   Test case

Reliable statements about the behaviour of bentonite as sealing and backfill material in a repository on the basis of the alternative conceptual model will only be possible once it has been demonstrated that the approaches are also useful for repository conditions. It also has to be possible to simulate re-saturation under increased hydraulic pressure levels as well as under non-isothermal conditions. The aspect of "re-saturation under increased hydraulic pressure levels" was analysed as part of the work related to the current EBS Task Force of SKB and UPC.

It was found that a re-saturation experiment that was chosen as a test case and performed by CIEMAT [23] and which is still underway was suitable for this purpose. In this experiment – as in the experiments in [13] – a bentonite test body is put in a cylindrical hollow steel form (diameter 7 cm, length 40 cm) and re-saturated from one of the two ends with liquid water. The test body in the CIEMAT experiment is slightly bigger, and FEBEX bentonite is used instead of the MX-80 variety. Still, the principle of one-dimensional re-saturation of compacted bentonite is the same as in [13]. Both experiments develop isothermally. The main difference consists of the fact that in the CIEMAT experiment the inflowing water is subjected to a pressure of 1.2 MPa. Temperature and relative humidity are constantly measured in three different locations inside the test body. The total amount of water absorbed is monitored, too, although these data are referred to as being "not totally reliable" [23].

5.2   Conceptual model under increased hydraulic pressure

As it proved to be possible to describe successfully the re-saturation experiments under laboratory conditions with the help of the empirical "diffusion law", the thought initially prevailed during the mid-1980s that the re-saturation process was driven by the gradient of the water content [2]. However, this notion was not confirmed for experimental conditions as encountered in a repository, i. e. for increased hydraulic pressure levels or higher temperatures. The alternative conceptual model shows how re-saturation under increased pressure and the empirical "diffusion law" can still be compatible.

What is decisive in this connection is the short initial phase in which the liquid water penetrates effectively into the bentonite. At atmospheric pressure, the interface between water and air reaches a penetration depth of approx. 4 mm [13] until an equilibrium sets in between the advective flow though the swollen bentonite and the vapour transport in the free pore space. According to the conceptual model, the penetration depth of the interface between air and water should in contrast increase at heightened hydraulic pressure. Otherwise, though, nothing changes compared with re-saturation under laboratory conditions. It therefore remains to be clarified where exactly the interface is in the CIEMAT experiment.

If one assumes as an ideal that the pressure gradient in the edge zone saturated with water is constant, the flow resistance increases linear to the penetration depth:

$$\Delta p = \frac{\Phi \, \eta \, \Delta x}{k} v \qquad\qquad (5.1)$$

p - hydraulic pressure [Pa]

Φ - porosity [-]

η - viscosity [Pa s]

k - permeability [m²]

v - velocity [m/s]

If the penetration depth for water at atmospheric pressure lies at 4 mm, a twelve-fold water pressure will therefore result in a penetration depth of 48 mm. This value is in fact confirmed if one looks at the humidity data of the experiment.

Fig. 5.1 shows the measured relative humidity as a function of the distance from the inflow boundary. The different humidity values measured at a certain time are linked by straight lines and show that the curvilinearity of the humidity distribution apparently decreases with time. According to the model representation, the position of the interface is expected at the point where humidity reaches the value of saturation. This point is approximated in Fig. 5.1 by linear extrapolation of the data of the two sensors closest to the inflow boundary up to a value of r_h=1. Since the curvilinearity of the humidity distribution decreases with time, the accuracy of this extrapolation increases with the modelling time. The point of intersection of the extrapolated lines with the saturation level converges after some time at about 5 cm, being in good agreement with the earlier

estimated value of 48 mm and thus providing a good indication of the position of the interface.
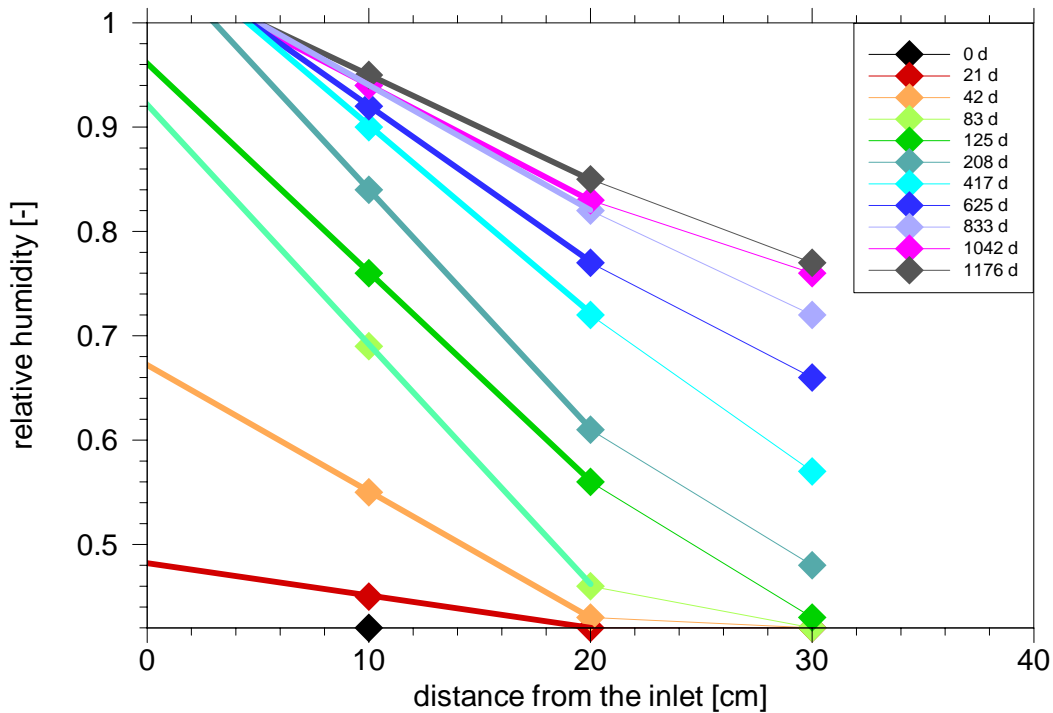

Fig. 5.1   Relative humidity as a function of the distance from the inflow boundary, and extrapolation of the values for the CIEMAT experiment.

The assumption is that the penetration of the liquid water phase takes place instantaneously. As a result of these considerations, the length of the bentonite test body in the vapour transport model is shortened by 5 cm compared to the length used in the experiment.

5.3   Modelling with VAPMOD

Re-saturation with consideration of the hydration kinetics is modelled with VAPMOD. The parameters that were used are summarised in Tab. 5.1. The coefficient for the binary gas diffusion of water vapour depends on pressure and temperature and was calculated according to [22]:

$$D = D^0 \, \frac{p^0}{p} \left(\frac{T}{T^0} \right)^{\Theta}$$

$\qquad\qquad\qquad\qquad\qquad\qquad\qquad\qquad\qquad\qquad$ (5.2)

D - coefficient of binary gas diffusion [m²/s]

T - temperature [K]

Θ - constant fit parameter [-]

(superscript index 0 indicates reference conditions)

Tab. 5.1   Parameters for the simulation of the CIEMAT experiment with VAPMOD.

Parameter	Value	Source
Initial density of the bentonite	1650 kg/m³	[23]
Final porosity	11 %	(assumption)
Particle density	2700 kg/m³	[23]
Tortuosity	0.4	(assumption)
Initial water content	13.7 %	[23]
Final water content	24.3 %	(derived from [23])
Reference hydration rate	10^{-6} 1/s	(estimated, cf. Ch. 3.1.3)
Temperature	21 °C	[23]
Molar mass of the water	18.016 g/mol	
Vapour saturation partial pressure	2230 Pa	
Atmospheric pressure	101325 Pa	
Binary gas diffusion coefficient	$2.13 \cdot 10^{-5}$ m²/s	(according to [22])

The results of the re-saturation experiment of CIEMAT are given in the form of relative humidities. VAPMOD provides the resulting humidities in the pore space, too, thus allowing a direct comparison of the results of measurement and model calculation, as shown in Fig. 5.2.

Although the diffusion-like character of the re-saturation process is simulated by the VAPMOD model, it is not possible to reproduce the measured data to a satisfactory degree. It appears that re-saturation does not take place fast enough in the model. As according to Ch. 4.1 the limiting factor is vapour transport, the reason could be that vapour transport is not adequately described. It has already been suggested in [13] that taking Knudsen diffusion into account may be a possible improvement.

Furthermore, gas pressure is assumed to be constant in the model. If, however, the inflow side is gas-tight due to the complete wetting with water, the gas pressure increases with the swelling of the clay minerals and with the corresponding reduction of

the pore space. According to equation (5.2), the diffusion coefficient increases in this connection with progressing re-saturation, which would qualitatively also occur in addition if Knudsen diffusion were considered.
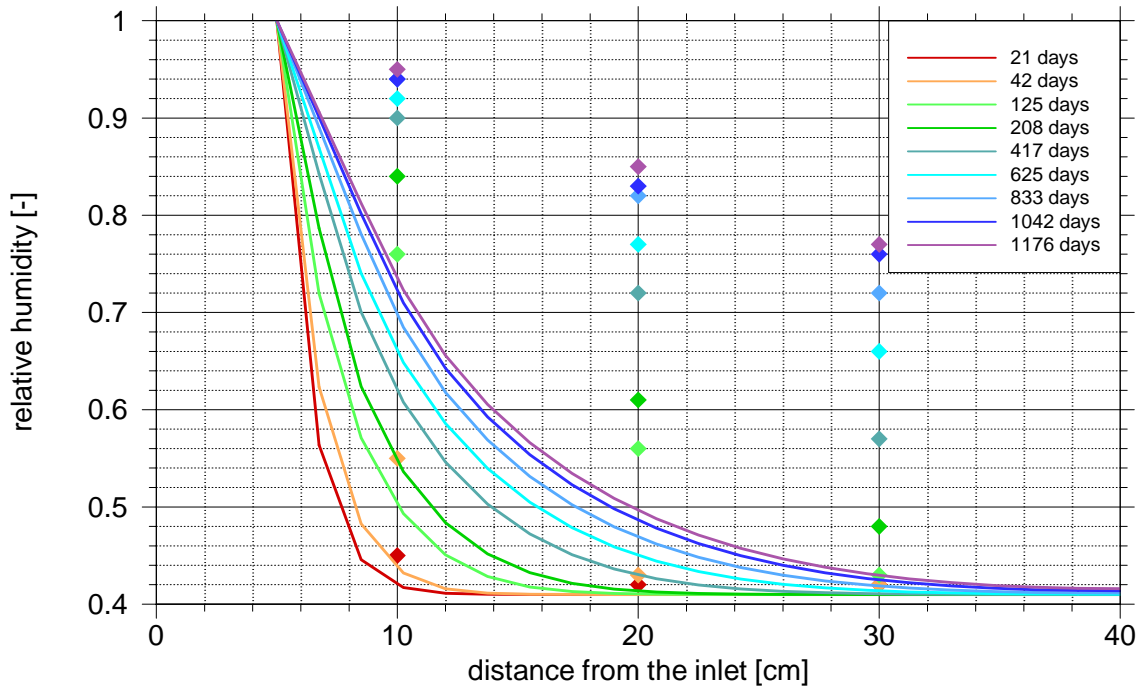

Fig. 5.2   Relative humidity; values measured and calculated with VAPMOD; square symbol: measurement, line: calculation.

5.4   Simplified balance equation

The data that are needed for the calculation of the CIEMAT experiment with the simplified balance equation are summarised in Tab. 5.2. The results are shown as local distributions (Fig. 5.3), breakthrough curves (Fig. 5.4) and as time-dependent water uptake (Fig. 5.5) distributions.

Tab. 5.2   Parameters for the simulation of the CIEMAT experiment with the simplified balance equation

Parameter	Value	Source
"Diffusion coefficient"	$6 \cdot 10^{-10}$ m²/s	(Data fit)
Initial density of the bentonite	1650 kg/m³	[23]
Particle density	2700 kg/m³	[23]
Water density	1000 kg/m³	
Initial water content	13.7 %	[23]
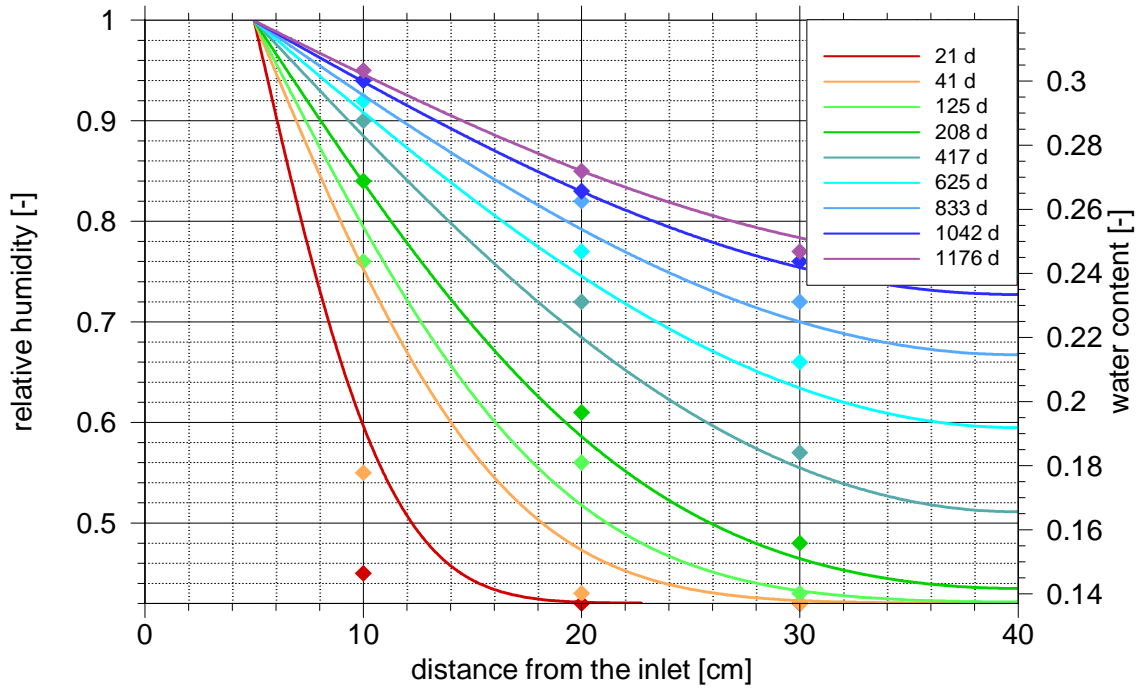
Fig. 5.3   Humidities from measurement and simplified balance equation; local distributions at different points in time; square symbol: measurement, line: calculation.

The calculated humidity distributions apply very well to large parts of the experiment. In the first months, however, the deviations are still quite large. One reason for this may be that an expanded transition zone with variable water content distribution may have formed during the first minutes of water injection since narrow pore channels will close faster than wide pores. In this case, the water in the transition area would first have to relocate before forming a constant flow of water and thus a uniform water front.

In the representation of the breakthrough curves, the initial deviations have a lesser weight so that the agreement of experiment and model appears even slightly better than with the spatial distributions. In all, agreement is not quite as convincing as in the case of the experiments with constant pressure (cf. Fig. 4.5).
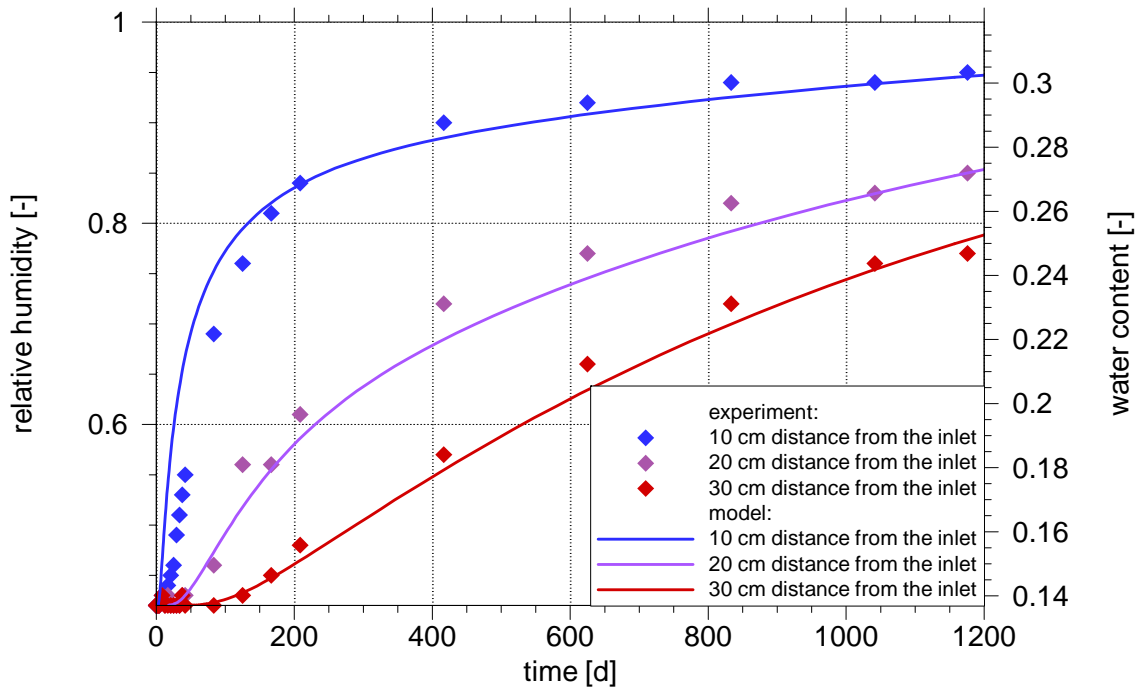
Fig. 5.4   Humidities from measurement and simplified balance equation; breakthrough curves.

The water uptake data indicate a possible explanation as they show irregularities that are difficult to interpret. Following an initial fast water uptake, the water uptake curve runs qualitatively like the calculated distribution for about 5 days. Here, the calculated values are as expected lower than the measured values as the initial water uptake is not taken into account in the model.

After that, however, there is for a limited time an unexplained further increase in the water uptake rate. Such phases of increased water uptake occur repeatedly during the course of the experiment, as the sectional graphs in Fig. 5.5 show. As the experiment is still continuing, the cause of this strange behaviour cannot yet be clarified.
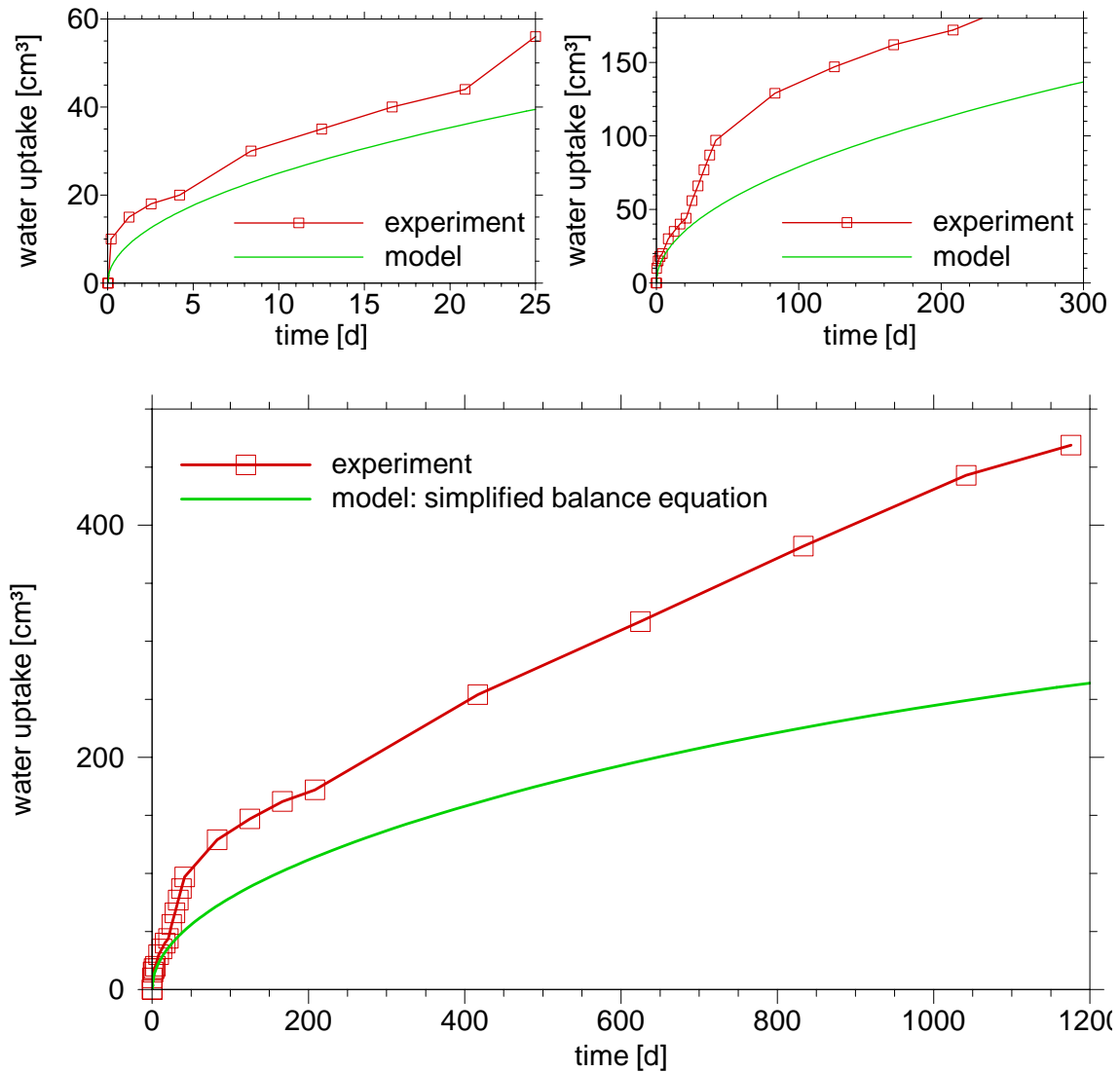
Fig. 5.5   Water uptake from measurements and simplified balance equation; representation showing different time periods.

As a result of geometrical considerations, the initial pore volume is calculated at 406 cm³. Even though re-saturation has not finished, a water uptake of 469 cm³ has already been measured. It may therefore be that a leakage in the experiment set-up is responsible for this irregular distribution of the measured data.

It is self-evident to assume that the quality of the measured data has suffered from this effect. Under these circumstances the agreement of modelling results and measured data – shown in Fig. 5.3 and Fig. 5.4 - appears satisfactory.

6   Summary and outlook

Even though the kinetics of the water uptake of bentonite from the gaseous water phase is an essential point in the modelling of re-saturation, only little has so far been known about it. Analytical functions were therefore developed from various different re-saturation experiments with water vapour which can be used to indicate the hydration rate as a function of the water content. The evaluation shows that with freely swelling pores, the hydration rate does not depend on the degree of compaction. If swelling is constrained, however, the hydration rate is reduced considerably. It is as yet unresolved what causes this effect and how it can be quantified.

Therefore, by way of trial, a water-content-dependent hydration rate was derived on the basis of the data of a re-saturation experiment involving water vapour in which the hydration rate decreases with increasing water content. Subsequently, the same experiment was simulated on the basis of this hydration rate. Modelling re-saturation via water vapour is still not satisfactory even with the help of the calibrated hydration rate. Compared with the theoretically derived hydration rates, however, the calibrated function yields a better reproduction of the measured values. Naturally, there is good agreement of measurement and model in the locations from where the data for the calibration originate. However, the discrepancies increasing with growing distance show that apart from hydration, the other major process involved in re-saturation – the transport of water within the pore space – may possibly not yet be covered correctly.

Thus the modelling of bentonite re-saturation with consideration of the hydration kinetics still has two gaps. First, the influence of the degree of compaction on the hydration rate has to be taken into account. Second, the question of a comprehensive description of water transport within the pore space has to be solved. However, it also turned out that the hydration rate is very high compared with the transport velocity of the water in the pore space. Hydration kinetics play therefore no major role in this process.

A conceptual model also exists for the re-saturation of compacted bentonites with liquid water. This model explains the re-saturation within the bentonite body mainly by vapour transport in the pore space and by hydration. By realistic simplifications, but especially by the assumption of instantaneous hydration, it is possible to transform the corresponding balance equation for the water formally into the well-known empirical

"diffusion law". It has been known of this empirical "law" for some time that it describes the re-saturation of bentonite under laboratory conditions well, with regard to water uptake rates as well as time-dependent water content distributions. So far, however, it has only been possible to calculate the empirical "diffusion coefficient" experimentally. Now this coefficient can be calculated with the help of the alternative approach – which rests on physical processes – from already well-known parameters, without having to rely on calibration parameters. In an example considered in this study, this coefficient lies within the very narrow limits that were found for the empirical "diffusion coefficient".

As a result, one can derive two things:

–   The formal agreement of the empirical findings and the physically justified model corroborates once more the assumption that re-saturation in a bentonite that is in contact with liquid water is mainly governed not by a liquid flow but by vapour diffusion within the pore space.

–   Up to now, the empirical "diffusion law" has not proved adequate for experimental conditions that deviate from laboratory conditions, especially from room temperature. The new theoretical approach could eliminate this deficiency by using a physically justified "diffusion coefficient" provided that the assumption of approximately instantaneous hydration also applies to increased temperatures and pressures.

A first step in the direction of a demonstration of the applicability of this simple conceptual model to situations relevant to a repository was the modelling of isothermal re-saturation experiments with liquid water under increased pressure. In this context it was possible to reproduce the experimental results well with the help of the "diffusion law" or the simplified balance equation for water vapour. What was decisive for the success was that the alternative conceptual re-saturation model is based on an initial condition that is different from earlier modelling attempts.

It thus only remains to verify the approaches with regard to non-isothermal conditions. (With a view to obtaining the highest possible reliability of the results, this work should be preceded by an investigation of re-saturation under increased constant temperatures before turning to non-isothermal conditions.) Should the approach with approximately instantaneous hydration also be confirmed under these conditions, it would also be

applicable under repository conditions. Compared with the established coupled THM models, this would simplify the description of re-saturation a great deal. Upon modelling the hydraulic processes, the numerical efforts as well as the efforts concerning the determination of parameters would be much less than with a two-phase-flow approach. A structure-mechanical calculation would be unnecessary.

However, as long as the effective water transport process has not been explained unequivocally, the question remains to be answered whether the use of the two-phase-flow approach in the hydraulic part of the established coupled thermal-hydraulic-mechanical (THM) models is appropriate. If not, this would put the applicability of these models to physically new issues into question. It therefore appears urgently necessary to clarify the physical basics of bentonite re-saturation.

References

[1]   Buhmann, D., Becker, D.-A., Keesmann, S., Kröhn, K.-P., Rübel, A.: Aktualisierung sicherheitsanalytischer Rechenprogramme für Teilsysteme eines Endlagers. Abschlussbericht des BMWA-Vorhabens 02 E 9178, GRS-Bericht GRS-200, 2004.

[2]   Börgesson, L.: Water Flow and Swelling Pressure in Non-Saturated Bentonite-Based Clay Barriers. Clay Barriers for Isolation of Toxic Chemical Wastes, International Symposium, May 28-30, Stockholm, 1984

[3]   Börgesson, L.: Persönliche Kommunikation, 2001.

[4]   Bucher, F., Müller-Vonmoos, M.: Bentonite als technische Barriere bei der Endlagerung hochradioaktiver Abfälle. Mitteilungen des IGB der ETH Zürich, Heft 133, S 51-64, 1987.

[5]   Carslaw, H.S. and Jaeger, J.C.: Conduction of Heat in Solids. 2. Auflage, Oxford University Press, 1959.

[6]   Helmig, R.: Multiphase Flow and Transport Processes in the Subsurface. Springer Verlag, 1997.

[7]   Japan Nuclear Cycle Developement Institute JNC: H12 : Project to Establish the Scientific and Technical Basis for HLW Disposal in Japan - Project Overview Report. JNC Report JNC TN1410 2000-001, 2000.

[8]   Johannesson, L.-E., Börgesson, L., Sandén, T: Backfill Materials Based on Crushed Rock (Part 2), Geotechnical Properties Determined in Laboratory. SKB, International progress report SKB-IPR-99-23, 1999.

[9]   Kahr, G., Kraehenbuehl, F., Müller-Vonmoos, M., Stoeckli, H.F.: Wasser-aufnahme und Wasserbewegung in hochverdichtetem Bentonit. NAGRA, Technischer Bericht 86-14, 1986.

[10]   Kröhn, K.-P.: New conceptual models for the resaturation of bentonite. Proceedings of the Workshop on "Clay Microstructure and its Importance to Soil Behaviour" held in Lund, 2002, Applied Clay Science, Vol. 23, 2003.

[11]   Kröhn, K.-P.: Investigation of uncertainties in the re-saturation model of bentonite as near-field buffer in a spent fuel repository in granite. Proceedings of the GRS/IRSN conference EUROSAFE, seminar 3, Paris 2003

[12]   Kröhn, K.-P.: Results and interpretation of bentonite resaturation experiments with liquid water and water vapour. in: Schanz, T.: Unsaturated Soils: Experimental Studies. Proceedings of the International Conference "From Experimental Evidence towards Numerical Modelling of Unsaturated Soils", Weimar, 2003, Springer, 2004.

[13]   Kröhn, K.-P.: Modelling the re-saturation of bentonite in final repositories in crystalline rock. Abschlussbericht des BMWA-Vorhabens 02 E 9430, GRS-Bericht GRS-199, 2004.

[14]   Kröhn, K.-P.: Proposal of an alternative re-saturation model for bentonite buffers - the conceptual model, the numerical model and the data base. In: Proceedings zum "Meeting on buffer & backfill modelling" in Lund. SKB-Bericht IPR-04-23, 2004.

[15]   Kröhn, K.-P.: New Evidence for the Dominance of Vapour Diffusion During the Re-saturation of Compacted Bentonite. Engineering Geology, Volume 82, Issue 2, 2005.

[16]   Massmann, J.W.: Applying groundwater flow models in vapour extraction system design. Journal of Environmental Engineering, 115(1), 1989.

[17]   Mooney, R. W., A., G. Keenan und L. A. Wood: Adsorption of Water Vapour by Montmorillonite; I: Heat of Desorption and Applicatioin of BET Theory. Journal of the American Chemical Society, Vol. 74, No. 6, 1952.

[18]   Pusch, R.: Water uptake, migration and swelling characteristics of unsaturated and saturated, highly compacted bentonite. KBS Report 80-11, SKBF, Stockholm, 1980.

[19]   Pusch, R., Muurinen, A., Lehikoinen, J., Bors, J., Erikson, T.: Microstructural and chemical parameters of bentonite as determinants of waste isolation efficiency. EUR 18950 EN, Luxemburg 1999.

[20]   Pusch, R., Kasbohm, J.: Can the Water Content of Highly Compacted Bentonite be Increased by Applying a High Water Pressure? SKB, Technical Report 01-33, 2001.

[21]   Pusch, R., Yong, R.: Water saturation and retention of hydrophilic clay buffer - microstructural aspects. Proceedings of the Workshop on "Clay Microstructure and its Importance to Soil Behaviour" held in Lund, Applied Clay Science, Vol. 23, 2003.

[22]   Vargaftik, N.B., Vinogradov, Y.K., Yargin, V.S.: Handbook of Physical Properties of Liquids and Gases. Begell house, inc., New York, Wallingford (UK), 1996.

[23]   Villar, M.V., Martín, P.L., Barcala, J.M: Infiltration test at isothermal conditions and under thermal gradient. Technical report CIEMAT/DMA/M2140/1/05, CIEMAT, Madrid, 2005.

Table of Figures

List of Tables